THE ASTROPHYSICAL JOURNAL, 440:60–68, 1995 February 10
© 1995. The American Astronomical Society. All rights reserved. Printed in U.S.A.

A COMPARISON OF TWO ALGORITHMS FOR SIMULATING COLLISIONLESS SYSTEMS

SHUNSUKE HOZUMI[1] AND LARS HERNQUIST[2]
Board of Studies in Astronomy and Astrophysics, University of California, Santa Cruz, CA 95064
Received 1993 October 25; accepted 1994 April 20

ABSTRACT

Two completely different simulation algorithms are compared by applying them to the same stellar dynamical problems: one is a self-consistent field (SCF) method for solving Poisson's equation and the other is a phase-space method for integrating the collisionless Boltzmann equation. We consider simulations of spherical stellar systems which are initially far from equilibrium and relax to their final states by gravitational collapse. The initial conditions consist of either uniform-density spheres or nonequilibrium models having Plummer density profiles, in which velocity dispersions are assigned according to given virial ratios. If a few tens of radial expansion terms with hundreds of thousands of particles are used in the SCF code, excellent agreement is found between the results it generates and those obtained with the phase-space solver, provided that a sufficiently large number of grid cells are employed with the latter. These findings imply that for simulating collisionless systems over many dynamical times, the SCF approach based on sampling phase space is competitive with the approach treating phase space as a continuous fluid. The results of our tests make it possible to estimate the number of particles and basis functions required in situations like those modeled. Limitations of the SCF method and the choice of an optimal set of basis functions are also discussed.

Subject headings: celestial mechanics, stellar dynamics — galaxies: formation — methods: numerical

1. INTRODUCTION

In general, it is necessary to solve Poisson's equation numerically when simulating self-gravitating collisionless systems. One approach, termed the self-consistent field (SCF) method by Hernquist & Ostriker (1992, hereafter HO), owing to its similarity to Hartree-Fock techniques from quantum theory, calculates the gravitational field by expanding the density and potential in a set of basis functions. In particular, when the full spatial dependence of the potential and density is expanded, this scheme represents the gravity in a mean-field sense and, so, is closer in spirit to collisionless dynamics than other N-body algorithms in which particles interact with one another directly (for a discussion see, e.g., Sellwood 1987; Barnes & Hernquist 1992).

Although SCF methods cannot describe the small-scale structure of a stellar system unless a prohibitively large number of basis functions are used, they have several potential advantages over direct N-body methods when applied to collisionless dynamics. For example, SCF codes do not require the introduction of a softening length to smooth out local irregularities in the density arising from the use of finite numbers of particles. More important, the elegant structure of the SCF method makes possible highly efficient implementations of it on a variety of computer architectures. Preliminary tests of the HO algorithm on a Connection Machine 5 demonstrate the feasibility of simulations employing $\sim 10^8$ particles with existing hardware (Hernquist, Sigurdsson, & Bryan 1994; see Hillis & Boghosian 1993). Given the explosive growth of parallel computing and the perfectly scalable nature of the SCF approach, it seems likely that simulations with particle numbers comparable to the actual number of stars in galaxies will be possible in the near future.

In spite of such advantages, SCF methods have been used only sparingly in applications to stellar dynamics. In large measure, this may be due to the inflexibility of this technique, in that the basis set must be chosen so that the lowest order terms are capable of reproducing the global structure of the system under investigation. Recently, HO proposed a new set of basis functions whose lowest order members accurately describe galaxies obeying the de Vaucouleurs $R^{1/4}$ law in projection. Their basis set will be useful, therefore, for studying spheroidal objects like elliptical galaxies. Crude empirical tests of the SCF method when applied to systems in equilibrium were done by HO. However, the reliability of this technique for simulating the dynamical evolution of systems far from equilibrium has never been proved. Clearly, it is crucial to demonstrate that the SCF method can handle such cases in view of the fact that many interesting problems involve, e.g., the evolution of systems toward equilibrium.

Rigorous proofs of the reliability of numerical codes like the SCF method are generally not feasible for highly nonlinear problems. Fortunately, progress can be made by relying on empirical tests in which different techniques are applied to the same problem and comparing the results obtained with them in detail, as was done by Inagaki, Nishida, & Sellwood (1984) who studied the nonlinear evolution of thin stellar disks. For modeling collisionless systems, there is another approach which neither employs particles nor depends on a softening length: phase-space methods in which the collisionless Boltzmann equation is solved directly. As Fujiwara (1983) has demonstrated, although spherical symmetry is assumed, this method can describe the violent relaxation of stellar systems accurately in the sense that the results are not subject to random fluctuations. Since collisionless Boltzmann simulations are a limiting case of a particle-based scheme in which the particle number goes to infinity, their results can be used to measure the validity of the SCF method when a finite number of particles are used. In this paper, we compare the results of collapse simulations between the two methods to study the

[1] Visiting Researcher, Faculty of Education, Shiga University, 2-5-1 Hiratsu, Otsu 520, Japan; hozumi@lick.ucsc.edu.
[2] Alfred P. Sloan Foundation Fellow, Presidential Faculty Fellow; lars@lick.ucsc.edu.

© American Astronomical Society • Provided by the NASA Astrophysics Data System

reliability of the SCF method although we are forced to examine spherical symmetric systems owing to limitations of the computer memory necessary for the phase-space method. Our results show that for a few tens of expansion terms with hundreds of thousands of particles, SCF codes are capable of describing the dynamics of certain collisionless systems, even those that are initially far from equilibrium and which relax to an equilibrium state in a violent manner.

In § 2, the two simulation methods are briefly described. Empirical tests are presented in § 3, comparing the SCF and phase-space methods when applied to the collapse of uniform-density spheres. In § 4, we discuss the choice of basis sets using "cooled" Plummer models. Conclusions are given in § 5.

2. METHODS

The SCF method is discussed in detail by HO. Their basis functions are derived from the model for spherical galaxies proposed by Hernquist (1990). In some of the tests presented in § 4, we also employ the functions suggested by Clutton-Brock (1973, hereafter CB), which are based on the Plummer model for spherical stellar systems (Plummer 1911; Binney & Tremaine 1987). In this paper, we restrict ourselves to systems whose self-gravity is forced to be spherically symmetric, so that we can make precise comparisons between the SCF method and the phase space technique described below. In the SCF code, this is accomplished by retaining only the $l = 0$ terms in the expansion of the angular variables. All simulations except those in § 3.2 employ $N = 60{,}000$ particles of equal mass. The equations of motion are integrated in Cartesian coordinates using a time-centered leapfrog algorithm (e.g., Press et al. (1986) with a fixed time step.

To solve the collisionless Boltzmann equation directly, we use a numerical code developed by Fujiwara (1983) which evolves the system using a splitting scheme (Cheng & Knorr 1976), unless otherwise specified. In what follows, we use Fujiwara's coordinate system to describe phase space: radius r, radial velocity u, and angular momentum j. Then, the number of mesh points in his notation is $(N_r, N_u, N_j) = (150, 150, 30)$ except for the simulation presented in § 3.2. As for our SCF calculations, a fixed time step is used.

3. COLLAPSE OF UNIFORM-DENSITY SPHERES

3.1. *General Comparison*

In this set of tests, we show the gravitational collapse of uniform-density spheres of total mass M and radius R_0 with Maxwellian velocity distributions. For these objects, the distribution function, f, can be written

$$f = \left(\frac{3M}{4\pi R_0^3}\right)\left(\frac{1}{2\pi\sigma_0^2}\right)^{3/2} \exp\left[-\frac{(u^2 + j^2/r^2)}{2\sigma_0^2}\right]. \quad (3.1)$$

In reality, we removed escapers from the initial data for the SCF simulations while the exact values from equation (3.1) were assigned to the mesh points for the collisionless Boltzmann simulations. The velocity dispersion, σ_0, is assigned according to prescribed viral ratios, $|2T/W|_0$, where T is the total kinetic energy and W is the total gravitational energy. In practice, the velocity dispersions are calculated from $\sigma_0 = [(GM/5R_0) \times |2T/W|_0]^{1/2}$. We have examined cases where $|2T/W|_0 = 1/2$, 1/4, and 1/8. The unit of mass and the gravitational constant, G, are taken so that $M = 1$ and $G = 1$, respectively. The unit of length is determined from the relation such that $|2T/W|_0 \times R_0 = 1$. As Fujiwara (1983) argued in his appendix, this choice of R_0 leads to nearly the same core size in the relaxed systems after collapse. Therefore, we do not need to use small time steps for cold initial states. The time step, Δt, in both the methods is taken to be $\Delta t = 0.1$ for all the models.

In the SCF method, we set the length scale of the basis functions to be unity and, as a starting point, we adopt $n_{max} = 16$, where n_{max} is the maximum number of expansion coefficients in the radial direction. This relatively large n_{max} is forced upon us by the fact that uniform-density spheres are not well-described by the density profile corresponding to a de Vaucouleurs law. This point is illustrated in Figures 1*a* and 1*b*, where we compare the potential and radial acceleration, respectively, computed from the HO basis set for different n_{max} to the exact values for a uniform-density sphere. It is clear from Figure 1*a* that the choice $n_{max} = 16$ should be sufficient to represent the potential reasonably well, but that the error in the radial acceleration might be a cause for concern, as shown in Figure 1*b*. However, the inaccuracies in the radial acceleration are mostly

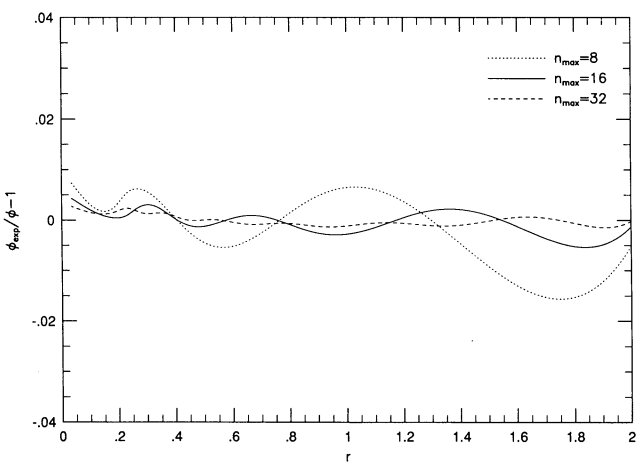

FIG. 1*a*

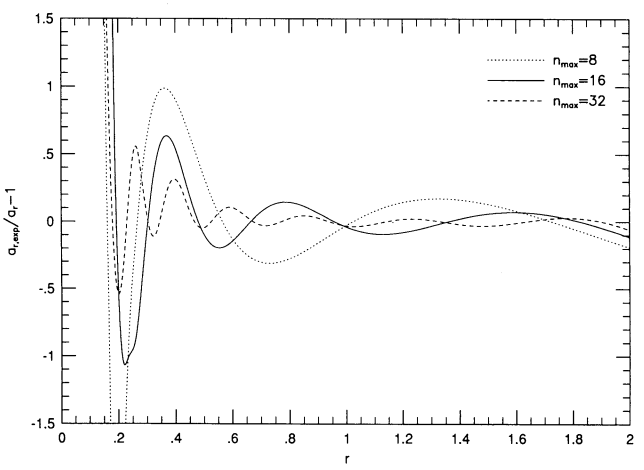

FIG. 1*b*

FIG. 1.—Relative error in the potential (*a*) and the radial acceleration (*b*) for a uniform-density sphere with $|2T/W|_0 = 1/2$ as a function of radius at $t = 0$. The figures compare the potential and acceleration, as computed with the HO basis functions for three different values of n_{max}, to their exact values for a uniform density sphere.

© American Astronomical Society • Provided by the NASA Astrophysics Data System

confined to small radii which contain relatively little mass. As we demonstrate below, the relatively crude representation of the force field near the center of the initial model has virtually no effect on the outcome of the collapse simulation.

With the above choice of time step, the maximum departures of the total system energy from its initial values were 0.18%, 1.0%, and 1.4% for $|2T/W|_0 = 1/2$, 1/4, and 1/8, respectively. The maximum errors occurred at the time of maximum collapse, and energy was conserved more accurately prior to and following this phase of the evolution, where energy was always conserved to better than 0.1% for the cases we considered. Although we tried the simulations for $|2T/W|_0 = 1/4$ and 1/8 with $\Delta t = 0.05$, we found practically no difference in the density profiles and the velocity dispersion profiles from the simulations with $\Delta t = 0.1$ except that the maximum energy errors were 0.25% and 0.36% for $|2T/W|_0 = 1/4$ and 1/8, respectively.

For the collisionless Boltzmann simulations, we used $R_{\min} = 0.1$, $U_{\max} = 2.1$, and $J_{\max} = 1.7$ in Fujiwara's (1983) notation. The radial velocity range of $(-U_{\max}, U_{\max})$ was sufficiently large that the stars which happened to gain large energy were not lost from the radial velocity boundaries. Mesh points were distributed out to maximum radii of $R_{\max} = 16.9$, 24.4, and 32.3 for $|2T/W|_0 = 1/2$, 1/4, and 1/8, respectively. Conservation of total energy amounted to 0.29% for $|2T/W|_0 = 1/2$. The maximum energy errors were 2.99% and 29.2% for $|2T/W|_0 = 1/4$ and 1/8, respectively. The simulations with $\Delta t = 0.05$ for $|2T/W|_0 = 1/4$ and 1/8 gave nearly the same level of energy conservation: 3.00% for $|2T/W|_0 = 1/4$ and 29.1% for $|2T/W|_0 = 1/8$. For the latter case, we stopped the simulation at $t = 130$ because of large numerical diffusion in the distribution function. These relatively large errors are caused mainly by escapers, as Fujiwara (1983) pointed out in his appendix.

Figure 2 shows the final density profiles resulting from these three cases. As can be seen from this figure, the density profiles following the approach of the system to equilibrium obtained from the two methods are in good agreement. In fact, there is little difference for the model with $|2T/W|_0 = 1/4$. On the other hand, the density profiles with $|2T/W|_0 = 1/2$ and 1/8 have slight differences in the envelope and in the core. Nevertheless, these models suggest that the basis set adopted by HO does not prejudice the end state of the resulting objects by coercing the final state to have the appearance of the lowest order terms.

The maximum energy errors of the collisionless Boltzmann simulations tell us that the model with $|2T/W|_0 = 1/2$ has borne negligible escapers whereas some fraction of particles become unbound from the systems in the other two models. In fact, only the model with $|2T/W|_0 = 1/2$ has shown no escapers for the SCF simulations. Since the sparsely distributed mesh points at large radii in the collisionless Boltzmann simulations makes it difficult to calculate the fraction of escapers accurately, a comparison of the time evolution of the virial ratios is not meaningful for the models including escapers. Thus, we present in Figure 3 the time behavior of the virial ratio only for $|2T/W|_0 = 1/2$. It is found that the difference in the virial ratios between the two methods becomes large at $t \approx 22$, although roughly speaking, the two evolve similarly with time beyond this point. A more detailed comparison of the time evolution of the virial ratios is presented in § 3.2.

We should mention the oscillatory behavior of the virial ratio with time for the collisionless Boltzmann simulation. It was not observed in Fujiwara's (1983) results. This is because he used a rather small number of mesh points; typically, he chose $(N_r, N_u, N_j) = (45, 40, 20)$. This had the effect of quickly erasing the oscillatory behavior, since the repeated interpolation required by the splitting scheme artificially smoothed the distribution function.

Next, we show the final velocity dispersion profiles of the collapse remnants in Figure 4. Again the two methods are in good agreement, with the largest differences apparent for the model with $|2T/W|_0 = 1/8$. In particular, the dispersion in tangential velocity shows excellent agreement, which is explained by the fact that the angular momentum of each particle is strictly conserved in spherical systems.

3.2. *Detailed Comparison*

The collisionless Boltzmann approach we use does not suffer ill effects arising from a particular representation of the density field, unlike the SCF approach which samples phase space using particles. We expect that as the number of particles used in an SCF calculation is increased, the results should describe a real collisionless system with greater and greater precision. It is interesting to examine how this convergence is achieved, in detail, to determine how many particles are required for practical equivalence to the collisionless dynamics of collapsing objects. For a fixed number of expansion terms, the computation time of the SCF method is exactly linear in the particle

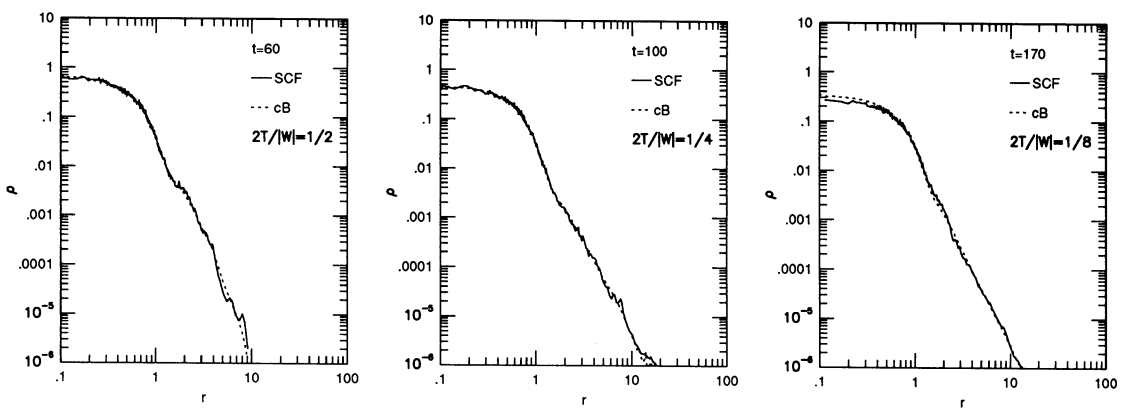

FIG. 2.—Final density profiles resulting from the collapse of uniform-density spheres with $|2T/W|_0 = 1/2$, 1/4, and 1/8. Solid lines are obtained with the SCF method, and the dashed lines from the collisionless Boltzmann simulations.

© American Astronomical Society • Provided by the NASA Astrophysics Data System

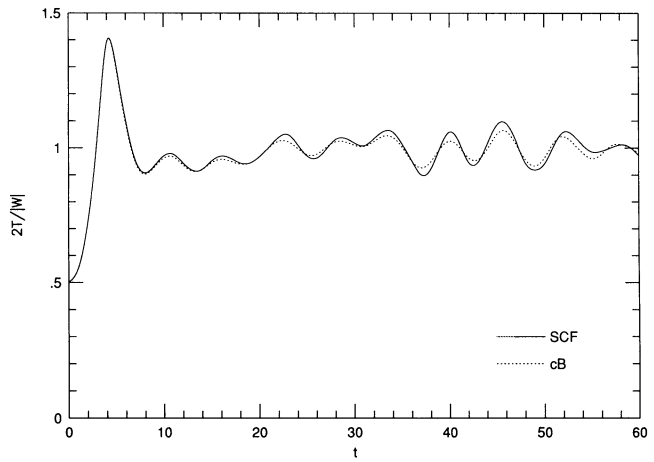

FIG. 3.—Time evolution of the virial ratios for the uniform-density sphere with $|2T/W|_0 = 1/2$. The solid line is obtained with the SCF method, and the dashed line from the collisionless Boltzmann simulation.

number, allowing us to span a large dynamic range in N. To quantify the convergence of the SCF method with changes in particle number, we focus on the time evolution of the virial ratio for $|2T/W|_0 = 1/2$, again using a time step $\Delta t = 0.1$.

After some trial and error, we also discovered that the collisionless Boltzmann simulations had to be refined since the time evolution of the virial ratio predicted by this approach had not converged fully. This results from the fact that the small-scale structure of phase space becomes increasingly important to the global evolution of the system as time proceeds, owing to phase mixing. The mesh employed by Fujiwara (1983) and in the tests reported above is not sufficient for this purpose. Recently, Fujiware & Hozumi (1994) developed a more sophisticated technique which combines the splitting scheme with a method devised by Rasio, Shapiro, & Teukolsky (1989). The key property of this algorithm is that the distribution function is evaluated by tracing the orbits of the stars on the grid points back to $t = 0$ periodically throughout the simulation, while the splitting scheme is used at times between those where orbit tracing is used. Since the distribution functions are provided analytically at $t = 0$, we can calculate them with arbitrary accuracy at such times when the orbit tracing is applied. We employed a grid with $(N_r, N_u, N_j) = (300, 300, 30)$ and carried out the orbit tracing at every 100 times steps (every 10 time units). The other parameters are $R_{\min} = 0.1$, $R_{\max} = 16.7$, $U_{\max} = 2.2$, and $J_{\max} = 1.7$.

We show in Figure 5 how the time evolution of the virial ratio obtained from the SCF method converges by varying N and $n_{\max}$. Except for the simulation with $N = 480{,}000$ and $n_{\max} = 8$, the behavior of the virial ratios with the SCF method is nearly identical to that from the collisionless Boltzmann simulation. Of course, the increase of $n_{\max}$ with a fixed N, or that of N with a fixed $n_{\max}$ gives better agreement. In particular, the case with $N = 960{,}000$ and $n_{\max} = 32$ is very close to the collisionless Boltzmann simulation except for the somewhat large difference after $t \sim 55$. Unfortunately, even the large number of mesh points in the collisionless Boltzmann simula-

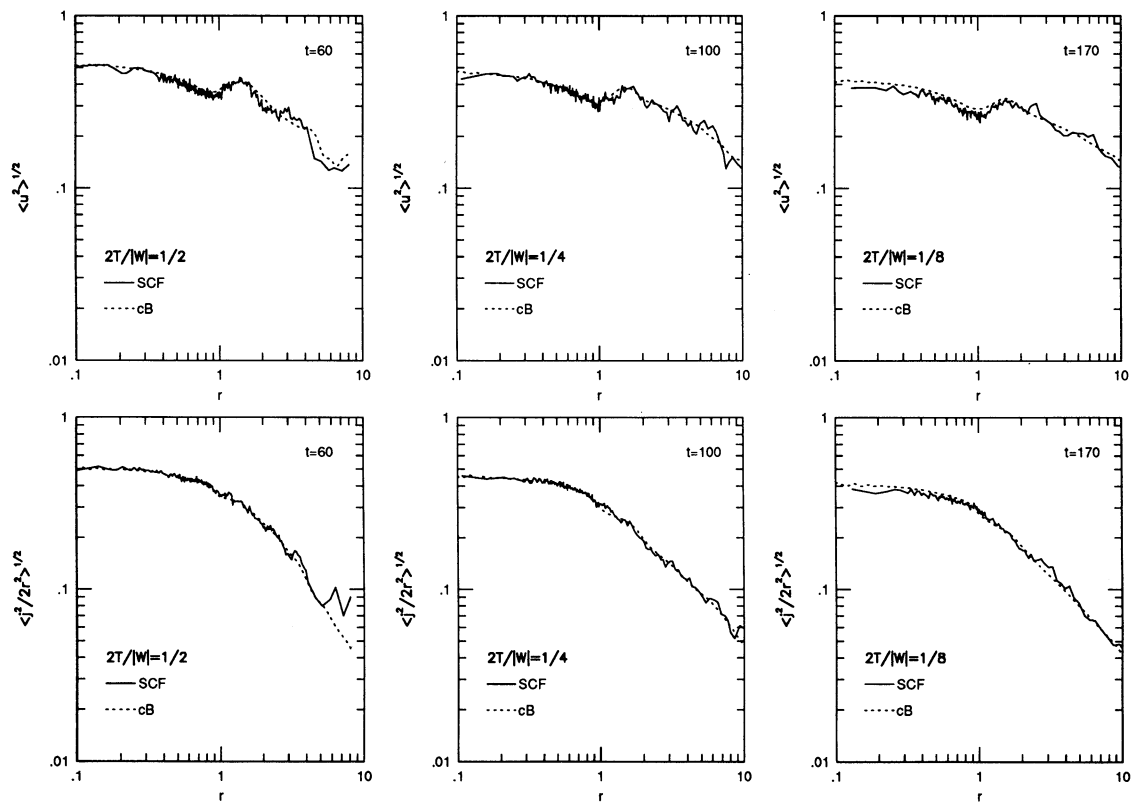

FIG. 4.—Final velocity dispersion profiles for the uniform-density spheres with $|2T/W|_0 = 1/2$, 1/4, and 1/8. Shown are the radial velocity dispersions $\langle u^2 \rangle^{1/2}$, and the tangential velocity dispersions $\langle j^2/2r^2 \rangle^{1/2}$. The solid lines denote the results with the SCF method, and the dashed lines those from the collisionless Boltzmann simulations.

© American Astronomical Society • Provided by the NASA Astrophysics Data System

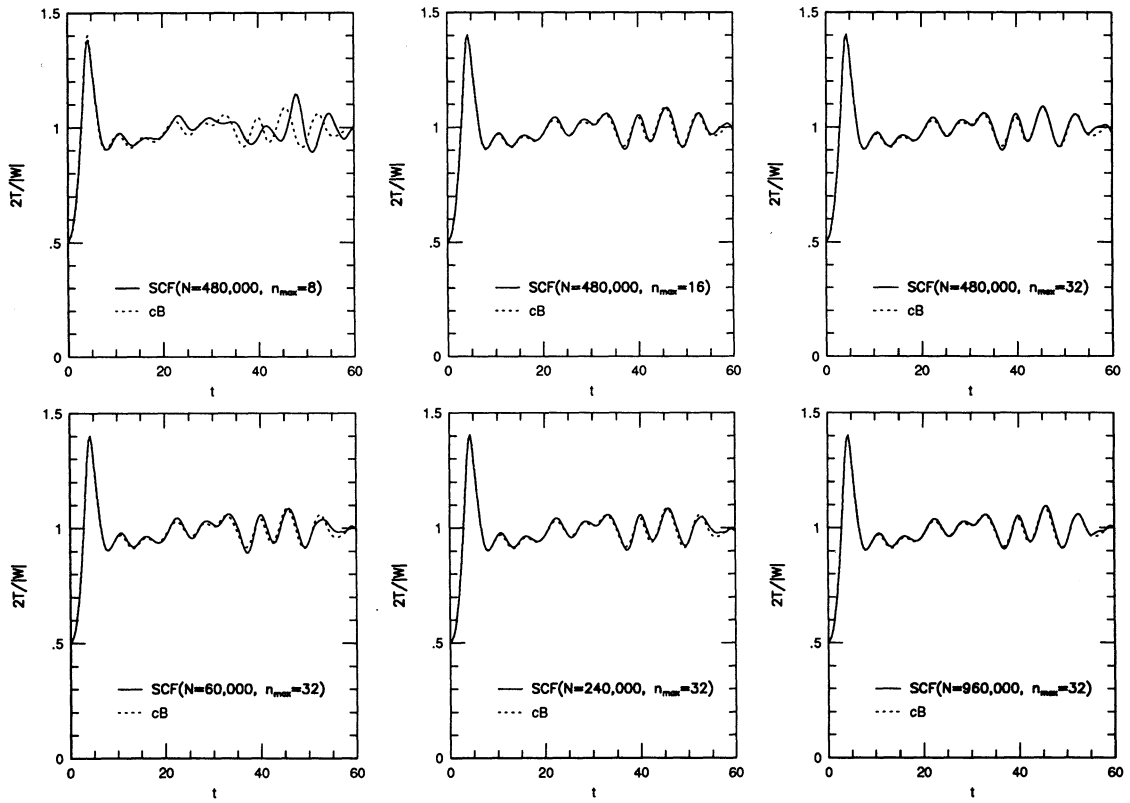

FIG. 5.—Same as in Fig. 3. The solid lines are obtained with the SCF method by varying n_{max} with a fixed N (*upper row*), and by varying N with a fixed n_{max} (*lower row*), while the dashed lines are from the collisionless Boltzmann simulation with the number of mesh points $(N_r, N_u, N_j) = (300, 300, 30)$ using the splitting scheme and the orbit tracing method.

tion became insufficient to describe the structures appearing in phase space after $t \sim 50$. Consequently, it is uncertain which method gives a better description of the actual dynamics after $t \sim 50$. As can be seen from Figure 5, the simulation with $N = 240{,}000$ and $n_{max} = 32$ practically gives the same behavior as that with $N = 960{,}000$ and $n_{max} = 32$ up to $t \approx 54$. Therefore, as far as simulations of spherical symmetric systems are concerned, the SCF method can reproduce the continuous limit to a high level of precision with hundreds of thousands of particles and a suitable choice of n_{max}. The results for $N = 60{,}000$ and $n_{max} = 32$ are only slightly worse, but do suggest that tens of thousands of particles per object are not sufficient if extremely high accuracy is required. We further conclude from Figure 5 that $n_{max} \approx 20$ is sufficient for simulations like those considered here except, again, if high precision is required.

4. COLLAPSE OF COOLED PLUMMER MODELS

In this section, we consider the effect of the choice of a basis set on the results of collapse simulations. We use Plummer models which have the density

$$\rho(r) = \frac{3M}{4\pi a^3}\left[1 + \left(\frac{r}{a}\right)^2\right]^{-5/2}, \tag{4.1}$$

and the potential

$$\Phi(r) = -\frac{GM}{a}\left[1 + \left(\frac{r}{a}\right)^2\right]^{-1/2}, \tag{4.2}$$

where M is the total mass. The units are such that $M = 1$ and $G = 1$. We determine the unit of length, a, from the relation such that $|2T/W|_0 \times a = 1$. The distribution function in equilibrium has the form

$$f(E) = K|E|^{7/2} \quad \text{for} \quad E < 0, \tag{4.3}$$

where E is the energy of a particle per unit mass, and K is a constant. To make the systems collapse, we follow the same procedure as Rasio et al. (1989): The systems are cooled by reducing the velocity dispersions from those in equilibrium in accord with the adopted values of $|2T/W|_0 = 1/2$, 1/4, and 1/8. The velocity dispersions are given by $\sigma_0 = [(\pi GM/32a) \times |2T/W|_0]^{1/2}$. The time-step is $\Delta t = 0.1$ for all the simulations shown here.

We perform the collapse simulations with the SCF method using the HO and CB basis sets. The length-scales implicit in both of the basis sets are set to be unity. For our initial models, the CB basis set should be suitable because the lowest member of this set is a Plummer model. We use $n_{max} = 6$ for $|2T/W|_0 = 1/2$ and 1/4, and $n_{max} = 16$ for $|2T/W|_0 = 1/8$. The maximum radii of the initial models are set to be $R_{max} = 17.5 \times a$ where the enclosed mass amounts to 99.5% of the total mass M. Energy was conserved to better than 0.04% for all the models, regardless of the basis set used.

We adopted $R_{min} = 0.1$, $U_{max} = 1.5$, and $J_{max} = 1.7$ for the collisionless Boltzmann simulations. The radial velocity range of $(-U_{max}, U_{max})$ was chosen so as not to lose the stars which gained large energy by chance. The maximum radii of the mesh points were taken to be $R_{max} = 38.4$, 64.3, and 153.3 for $|2T/W|_0 = 1/2$, 1/4, and 1/8, respectively. Conservation of total energy was achieved to better than 0.03%.

© American Astronomical Society • Provided by the NASA Astrophysics Data System

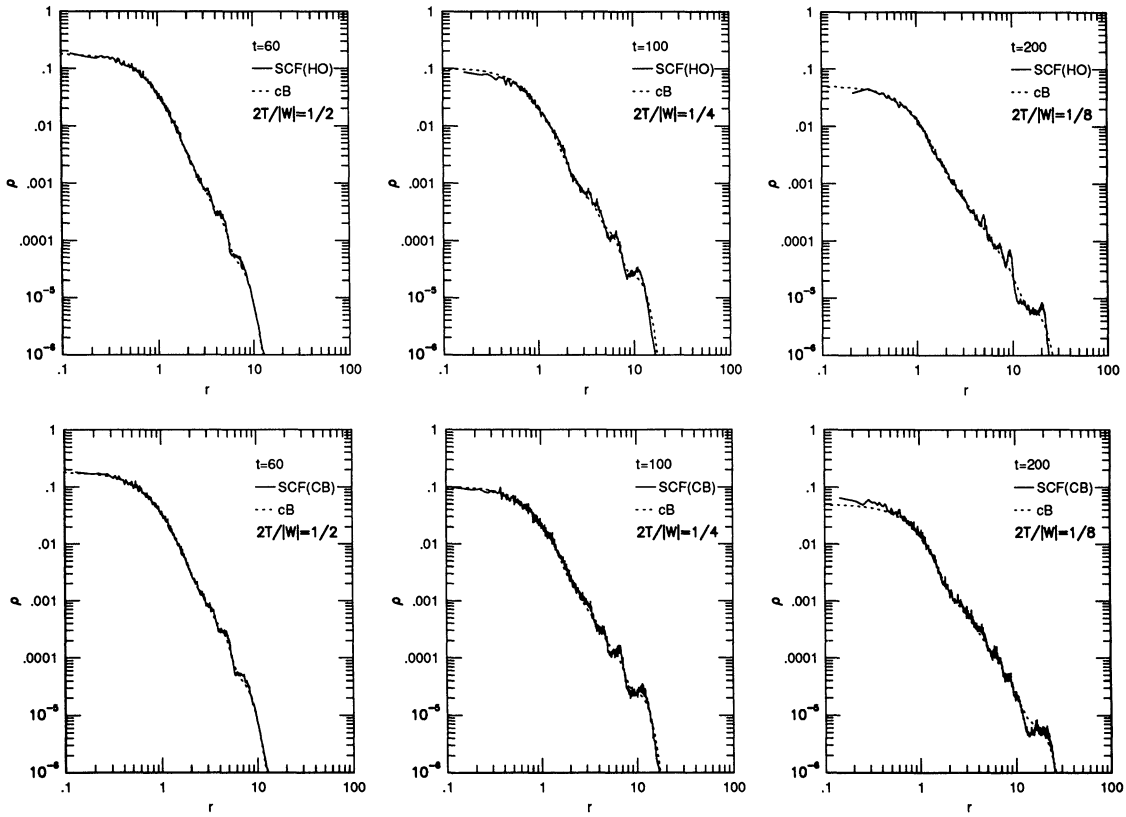

FIG. 6.—Final density profiles for the cooled Plummer models with $|2T/W|_0 = 1/2$, 1/4, and 1/8 using HO and CB basis sets. The solid lines are obtained with the SCF method, and the dashed lines from the collisionless Boltzmann simulations.

In Figures 6 and 7 we present the density profiles and the velocity dispersion profiles, respectively, in the relaxed states. The profiles for both the basis sets look very similar, and agree well with those found in the collisionless Boltzmann simulations. Thus, it is difficult to determine from these statistically averaged quantities if one or the other of the basis sets is more appropriate for such simulations.

The models studied here did not generate escaped particles, making it possible to quantify differences in the basis sets in terms of the time variation of the virial ratios; an example of which is shown in Figure 8. From these results, it appears that the HO basis set provides better agreement with the collisionless Boltzmann solver than the CB basis functions. For $|2T/W|_0 = 1/4$ and 1/8, the virial ratios obtained from the CB basis set deviate from the correct solution immediately following the time of maximum collapse. The consequences of these differences for the global structure of the system are illustrated in Figure 9, where the density profile near the time of maximum collapse for $|2T/W|_0 = 1/4$ is shown. The density profiles can be fitted to $\rho(r) \propto r^{\alpha}$ in the envelope. The power-law index is $\alpha \approx -3$ at around maximum collapse. Thus we expect that for fixed $n_{\max}$, the HO basis functions should give a better description of the resulting evolution since the density of the lowest member of HO basis set has the power-law index of -4 in the envelope while that of CB basis set has the power-law index of -5 (see eq. [4.1]). In addition, the HO basis set is better able to represent highly concentrated systems, as is the models here near maximum collapse, since the lowest order term has singular density at the origin.

It follows from the simulations shown here that a basis set which can well approximate the density profile of the relaxed state with only a few terms is desirable for collapse simulations.

5. CONCLUSIONS

We have studied the collapse of uniform-density spheres and cooled Plummer models to demonstrate the reliability of the SCF method for modeling the dynamics of collisionless systems initially far from equilibrium. We have shown that, in principle, this approach can successfully reproduce the time-evolution of such a system, when compared with results obtained with a method which solves the collisionless Boltzmann equation using a finite-difference scheme. With only a modest number of particles and basis terms, the SCF method can practically attain the continuous limit when predicting information such as density profiles and velocity dispersion profiles. In addition, if a sufficiently large number of particles are used, more detailed properties, such as the time evolution of the virial ratio can be reproduced almost exactly.

The success of simulations with the SCF method depends on the basis set chosen. As suggested in § 4, for collapse simulations like those reported here, the basis set should probably be selected so that the basis set gives an accurate description of the final relaxed state, rather than the initial conditions. One example of such a basis set is that suggested by HO, which is based on a galaxy obeying the de Vaucouleurs law in projection. As is well-known, collapse simulations typically produce end-states whose density profiles are well-described by $R^{1/4}$ laws in projection.

© American Astronomical Society • Provided by the NASA Astrophysics Data System

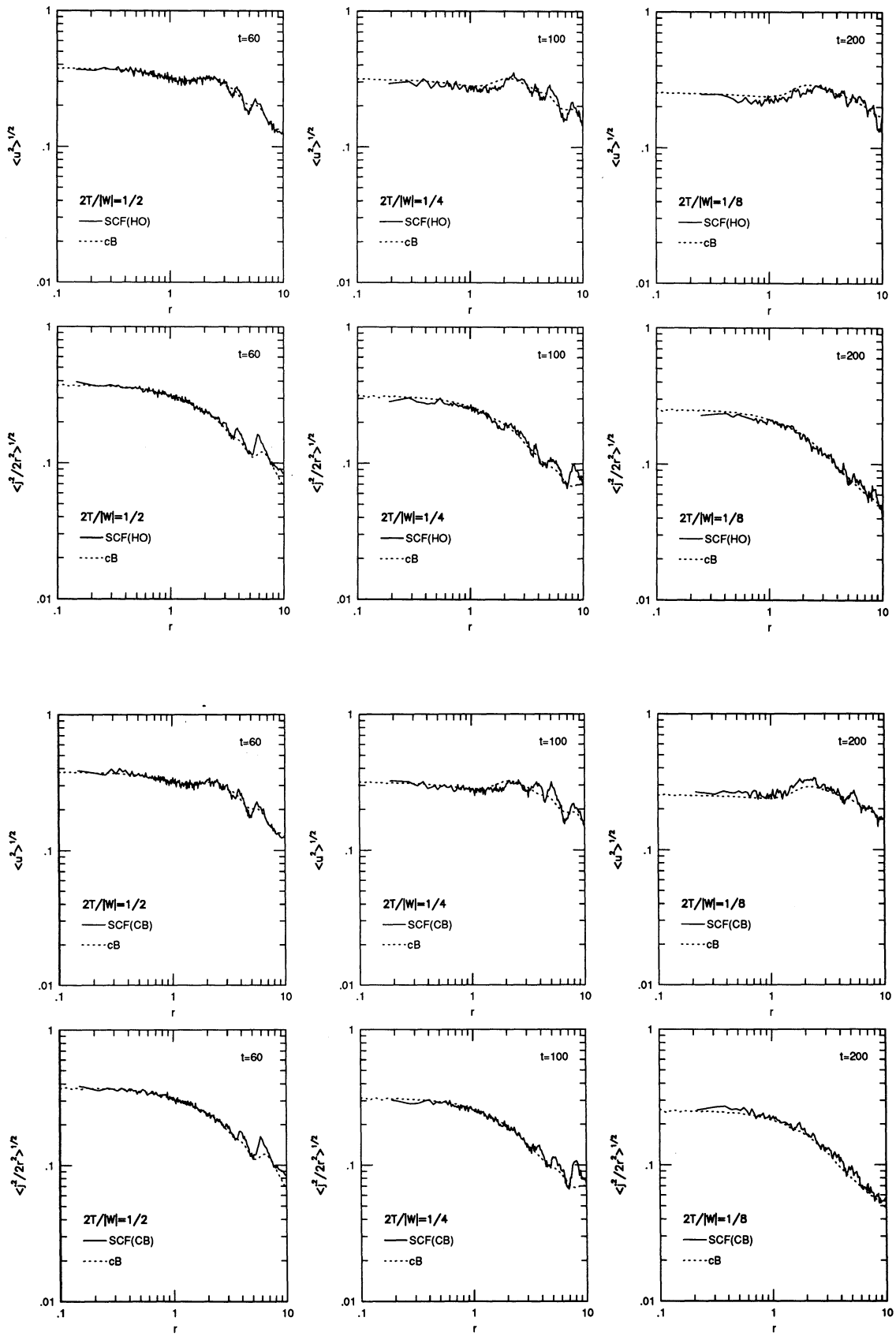

FIG. 7.—Final velocity dispersion profiles for the cooled Plummer models with $|2T/W|_0 = 1/2$, 1/4, and 1/8 using HO and CB basis sets. The symbols and the line types have the same meaning as in Fig. 4.

© American Astronomical Society • Provided by the NASA Astrophysics Data System

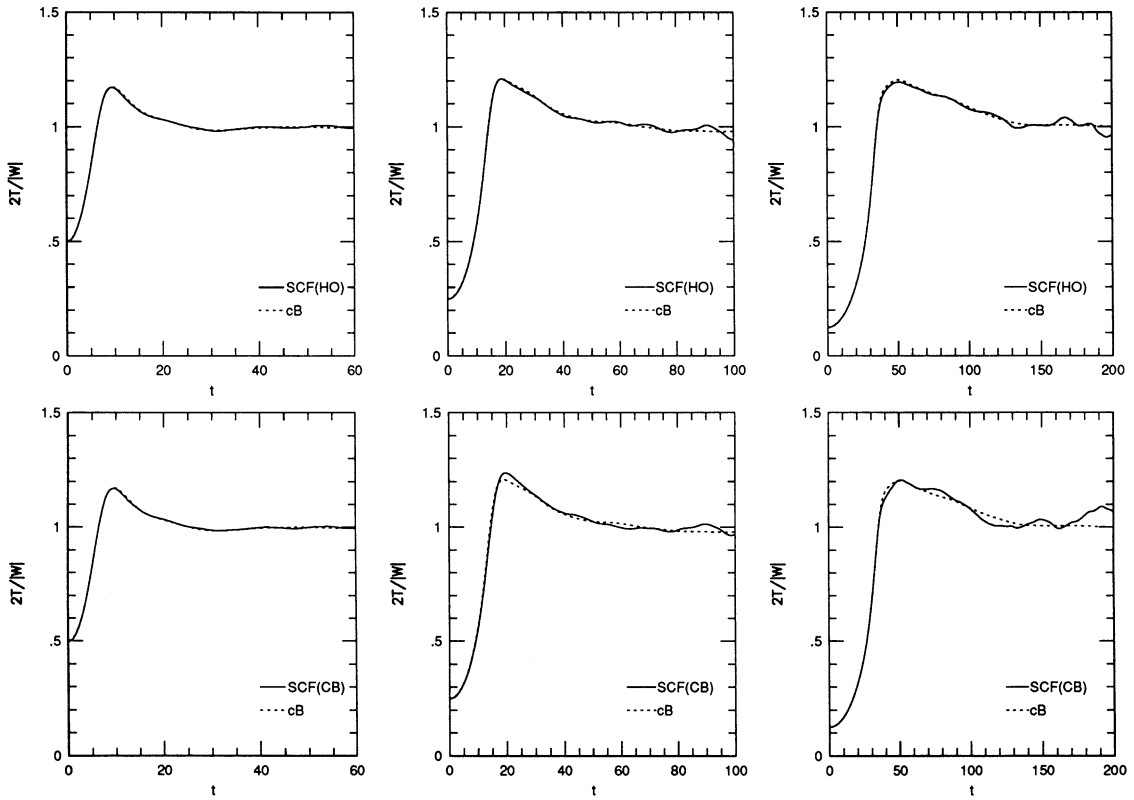

FIG. 8.—Time evolution of the virial ratios for the cooled Plummer models with $|2T/W|_0 = 1/2$, 1/4, and 1/8 using HO and CB basis sets. The solid lines are obtained with the SCF method, and dashed lines from the collisionless Boltzmann simulations.

Once a basis set is determined, the accuracy of the SCF method is determined by a suitable choice of the maximum number of expansion coefficients such as n_{max} and l_{max}, and the particle number. Clearly, the appropriate choices of n_{max}, l_{max}, and N are problem-dependent. Our results in § 3.2 suggest that even in some extreme cases values of n_{max} in the range 10–30 are adequate to describe the evolution of some nonequilibrium systems in detail if hundreds of thousands of particles are used.

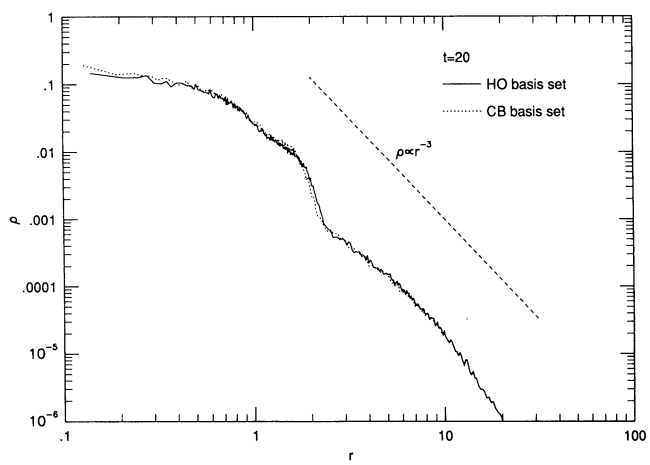

FIG. 9.—Density profiles for the cooled Plummer model with $|2T/W|_0 = 1/4$ at around the maximum collapse ($t = 20$). The solid line is obtained from HO basis set, and the dashed line from CB basis set.

In this paper, we have not explored departures from spherical symmetry. The SCF method is easily applicable to nonspherical symmetric systems while the application of the phase-space method is restricted to the systems with some kind of symmetry owing to memory limitations of presently available computers. Based on preliminary empirical tests, similar values of l_{max} to those of n_{max} will be required when the system is very nonspherical, implying that a total of several thousand expansion terms may be needed in some cases. Global properties can be reproduced, however, with fewer terms. Likewise, upwards of a hundred thousand particles may be required to follow the evolution of rapidly evolving systems. This is not specific to the SCF method, but is rather a fundamental limitation of the N-body approach. Given the efficient nature of the SCF method on parallel architectures, however, simulations with $N \gg 10^5$ are quite feasible.

We are very grateful to Takao Fujiwara for kindly providing us with his collisionless Boltzmann code and for valuable advice concerning its use. We also thank Jerry Sellwood for his critical reading of the manuscript as a referee. One of the authors (S. H.) would like to thank Lick Observatory for its hospitality throughout the research. This work was supported in part by the Pittsburgh Supercomputing Center, the Alfred P. Sloan Foundation, NASA grant NAGW-2422, and the NSF under grant AST 90-18526 and the Presidential Faculty Fellows Program.

© American Astronomical Society • Provided by the NASA Astrophysics Data System

REFERENCES

Barnes, J. E., & Hernquist, L. 1992, ARA&A, 30, 705
Binney, J., & Tremaine, S. 1987, Galactic Dynamics (Princeton: Princeton Univ. Press)
Cheng, C. Z., & Knorr, G. 1976, J. Comput. Phys., 22, 330
Clutton-Brock, M. 1973, Ap&SS, 23, 55 (CB)
Fujiwara, T. 1983, PASJ, 35, 547
Fujiwara, T., & Hozumi, S. 1994, MNRAS, submitted
Hernquist, L. 1990, ApJ, 356, 359
Hernquist, L., & Ostriker, J. P. 1992, ApJ, 386, 375 (HO)
Hernquist, L., Sigurdsson, S., & Bryan, G. 1995, ApJ, submitted
Hillis, W. D., & Boghosian, B. M. 1993, Science, 261, 856
Inagaki, S., Nishida, M. T., & Sellwood, J. A. 1984, MNRAS, 210, 589
Plummer, H. C. 1911, MNRAS, 71, 460
Press, W. H., Flannery, B. P., Teukolsky, S. A., & Vetterling, W. T. 1986, Numerical Recipes: The Art of Scientific Computing (Cambridge: Cambridge Univ. Press)
Rasio, F. A., Shapiro, S. L., & Teukolsky, S. A. 1989, ApJ, 344, 146
Sellwood, J. A. 1987, ARA&A, 25, 151

© American Astronomical Society • Provided by the NASA Astrophysics Data System